Folding and Unbinding Transitions in Tethered Membranes

FARID F. ABRAHAM AND MEHRAN KARDAR

Molecular dynamics simulations of tethered membranes indicate that an attraction between the monomers leads to a well-defined sequence of folding transitions with decreasing temperature. With insights gained from Landau theory and simulations of bimembranes, the folding transitions are found to be intimately linked to the unbinding of membranes. Finite-size effects, mainly due to the loss of entropy from edge fluctuations, play an important role in hindering folding transitions.

TETHERED MEMBRANES (*1*), WHICH are simple generalizations of linear polymers to two-dimensionally connected networks, have been the subject of much recent interest (*2*). Unlike polymers (*3*), tethered surfaces have a flat phase with long-range orientational order (*4, 5*). The presence of such a phase has several interesting consequences (*2, 4–6*), one of which is the novel folding transitions discussed here. In a poor solvent [as defined in (*3*)], there is an effective attraction between monomers of the network that increases with decreasing temperature. For polymers this leads to a transition between low-density (crumpled) and high-density (compact) phases at a so-called θ point (*3*). In contrast, the transition between flat and compact states of a membrane proceeds through a sequence of folding transitions. We argue that these transitions are intimately linked to the unbinding of membranes (*7*), the unbinding temperature being the limiting value of all folding temperatures for infinitely big surfaces. Finite-size effects, which are due to crease energies and, more important, to loss of entropy of edge fluctuations, play a crucial role in the behavior of finite-size membranes.

There are two clear motives for performing simulations of tethered surfaces with an attractive interaction in addition to the usual hard-core repulsion. First, although theoretical studies (*8, 9*) based on continuum models predict a transition between flat and crumpled membranes, most simulations of self-avoiding surfaces have observed only the flat phase (*10*). An attractive potential may partly overcome the entropic rigidity that is due to self-avoidance and lead to a crumpled phase. Second, the difficulty in obtaining compact surfaces by applying external pressures (*11*) or by regular foldings (*1*) suggests that it may be impossible to obtain a compact phase in a simulation. In fact, the simulations do find a compact state (*12*) in which the membrane mass M scales as $M \sim L^2 \sim R^3$, where L is the linear dimension and R is the radius of gyration. Recent experiments on graphite oxide membranes also indicate a compact phase in a poor solvent (*13*). Improving the quality of the solvent appears to result in crumpled membranes.

Molecular dynamics simulations were performed on the model of tethered membranes used by Abraham and Nelson (*12*). The nearest neighbor atoms are tethered into a triangular array with a potential including a strong repulsive component at short and long distances. Non–nearest neighbor particles interact through a Lennard-Jones potential and are terminated at separations greater than 2.5σ (σ is the interatomic separation at which the potential vanishes). At high temperatures the potential is irrelevant, and the membrane is flat as a result of entropic rigidity (*12*). The width H of the interface, however, scales with its linear size (*4–6, 12, 14*) as $H \sim L^{\zeta}$, where $\zeta \sim 0.65$. At low temperatures the membrane collapses into a compact phase characterized by a typical radius R that grows as $R \sim L^{2/3}$.

What happens at intermediate temperatures is best understood by examining Fig. 1, which depicts a hexagonal surface with L = 75 particles along the diagonal. On cooling, the membrane folds on itself once at a temperature $T_1(75) = 3.15 \pm 0.05$ (all temperatures are measured in units of the depth of the attractive Lennard-Jones potential). A crease neatly divides the membrane in half. The folded structure has roughly the same width as the unfolded one, so that the in-plane density is twice as big. On further cooling there is a second folding transition at $T_2(75) = 2.75 \pm 0.05$. There are now two orthogonal creases that divide the membrane into four roughly equal parts folded together. The density continues to increase on decreasing temperature, but it is difficult to identify any more distinct folding temperatures.

One can obtain an idea of the sharpness of these transitions by examining Fig. 2, which depicts the three moments of inertia as a

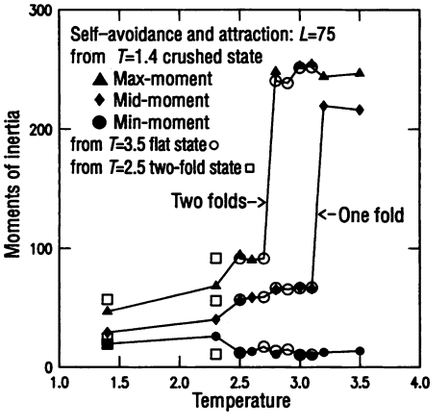

Fig. 2. The three moments of inertia as a function of temperature. The open symbols are for cooling from the flat phase, and the closed symbols are for heating from the collapsed state.

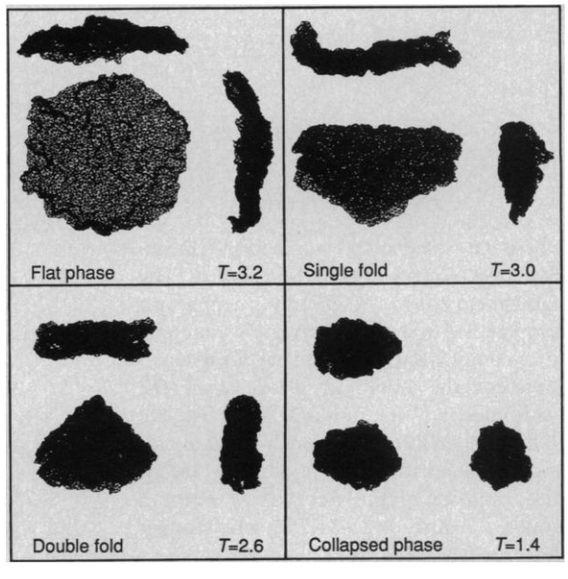

Fig. 1. Configurations of the membrane at temperatures T = 3.2, 3.0, 2.6, and 1.4 corresponding to flat, singly folded, doubly folded, and collapsed states, respectively. The perspectives are along the axis of the moment of inertia tensor.

F. F. Abraham, IBM Research Division, Almaden Research Center, San Jose, CA 95120.
M. Kardar, Physics Department, Massachusetts Institute of Technology, Cambridge, MA 02139.

function of temperature. On the first fold there is a reduction in the second moment of inertia roughly by a factor of 4, which is consistent with a single fold. The smallest moment of inertia does not change, suggesting that the thickness of the membrane does not change appreciably on folding. There is a somewhat smaller drop in the largest moment at the second folding transition. These transitions are also obtained by heating from the compact phase (*12*) at $T = 1.4$ (where $R \sim L^{2/3}$), as indicated by the filled-in symbols in Fig. 2. The reversible nature of the folding transition rules out the possibility that these are metastable configurations. By contrast, if we cool from the $T = 2.5$ double-fold state, the compact phase is not obtained (Fig. 2); that is, reversibility is not realized between the compact and double-fold states. Hence, although we are confident about the occurrence of the two folding transitions, it is impossible for us to establish the lowest free energy state at low temperatures ($T < 2.5$).

We can understand the above results in the context of a Landau theory of tethered surfaces (*9, 15*). This approach is in analogy with continuum statistical field theories of elasticity or magnetism. An effective free energy is constructed for $\mathbf{r}(x_1, x_2)$, which is a coarse-grain version of the coordinates $\mathbf{r}_{m,n}$ of the atoms in the network. On the basis of symmetry considerations, the lowest order terms in a gradient-density expansion for the Hamiltonian $\beta\mathcal{H}$ are (*9, 15*)

$$\beta\mathcal{H}[\mathbf{r}(\mathbf{x})] = \int d^2\mathbf{x} \left[\left(\frac{t}{2}\right)(\partial_i\mathbf{r} \cdot \partial_i\mathbf{r}) + u\,(\partial_i\mathbf{r} \cdot \partial_j\mathbf{r})\,(\partial_i\mathbf{r} \cdot \partial_j\mathbf{r}) + v\,(\partial_i\mathbf{r} \cdot \partial_i\mathbf{r})\,(\partial_j\mathbf{r} \cdot \partial_j\mathbf{r}) + \left(\frac{\kappa}{2}\right)(\partial_i^2\mathbf{r} \cdot \partial_j^2\mathbf{r}) \right] + \frac{b}{2}\int d^2\mathbf{x}\, d^2\mathbf{x}'\, \delta^3[\mathbf{r}(\mathbf{x}) - \mathbf{r}(\mathbf{x}')] + \frac{c}{6}\int d^2\mathbf{x}\, d^2\mathbf{x}'\, d^2\mathbf{x}''\, \delta^3[\mathbf{r}(\mathbf{x}) - \mathbf{r}(\mathbf{x}')]\, \delta^3[\mathbf{r}(\mathbf{x}) - \mathbf{r}(\mathbf{x}'')] \quad (1)$$

where $\partial_i\mathbf{r} = \partial\mathbf{r}/\partial x_i$ and summation convention over $(i,j) = (1, 2)$ is assumed. The parameters t, u, v, κ, b, and c depend on temperature and the microscopic potential in a complicated fashion. The local terms represent the nonlinear elasticity of the membrane, and the nonlocal terms are due to long-range interactions such as self-avoidance. If fluctuations are ignored, a mean-field estimate of the free energy F for a uniform density n ($\sim L^2/R^3$) and tangent vector $\mathbf{m}R^3(\sim R/L)$ is

$$\frac{\beta F}{L^2} = \min_{m,n} \left\{ \left[\frac{t}{2} m^2 + 2(u + 2v)m^4 \right] + \left(\frac{b}{2} n + cn^2 \right) \right\} \quad (2)$$

In the spirit of the Landau theory of magnetism, the signs of the lowest order terms (that is, t and b) determine the phase of the membrane. For positive t and b, $m = n = 0$ at the minimum, signaling the crumpled phase; in fact, a more precise treatment shows that as R and L go to infinity m and n do not go to 0 independently but rather so as to reproduce the Flory estimate (*1*) $R \sim L^{4/5}$. For $t < 0$ and $b > 0$, the order parameter m is nonzero, indicating the flat phase (*9*) ($R \sim mL$). If $b < 0$ and $t > 0$, m is 0, and the density n becomes finite ($L^2/R^3 \sim n$). This is the compact phase, and $b = 0$ is the analog of the θ point for polymers (*15*). Finally, for negative t and b, both m and n tend to be nonzero. If the energy cost of creases is ignored, this can be achieved by regularly folding the membrane into a compact structure. The resulting phase diagram is sketched in Fig. 3. [A previous study of this Landau theory (*15*) left out the possibility of a folded state and indicated a direct transition between the flat and compact phases in the $(t, b) < 0$ quadrant.] The simulation results indicate that on decreasing temperature the membrane proceeds along the trajectory indicated in Fig. 3. If there is also a crumpled phase, as suggested by experiments (*13*), it should be possible to devise a potential such that the flat-to-compact trajectory proceeds via the crumpled phase.

Finite-size effects play an important role in polymers and membranes and are integral to understanding the folded state. Although the surface tends to fold back and forth as much as possible, it must do so without tearing apart; the difficulty of finding the optimal folding soon becomes evident if one experiments with a sheet of paper. Nonetheless there are such foldings (*16*), and presumably a sufficiently big membrane will approximate them to some extent. At small sizes, the competition between the free-energy gain from folding ($\sim bL^2/2$) and the energy loss due to creasing ($\sim \epsilon_c L$) becomes important. For small $b < 0$, a finite membrane stays flat and folds only when b is sufficiently negative to compensate for the crease energy [at $b_1(L) \sim -\epsilon_c/L$]. The singly folded membrane is then stable as a result of the energy cost of creating a second crease, and b has to be reduced further to achieve a second folding transition at $b_2(L)$ (we shall see later that on including fluctuations the creasing energy is much less important). Therefore, at finite L there will be a sequence of folding transitions that converge on each other as $L \to \infty$. This is supported by simulations on membranes with $L = 49$, for which $T_1(49) = 2.90 \pm 0.05$ and $T_2(49) = 2.15 \pm 0.05$. At lower temperatures it becomes difficult to distinguish between a collapsed state and a folded state with a finite number of folds. More extensive simulations are necessary to establish definitely the occurrence of a collapsed state (*12*) from the double-fold or multifold regime. We shall instead focus on the critical behavior and finite-size scaling in the vicinity of the first folding transition.

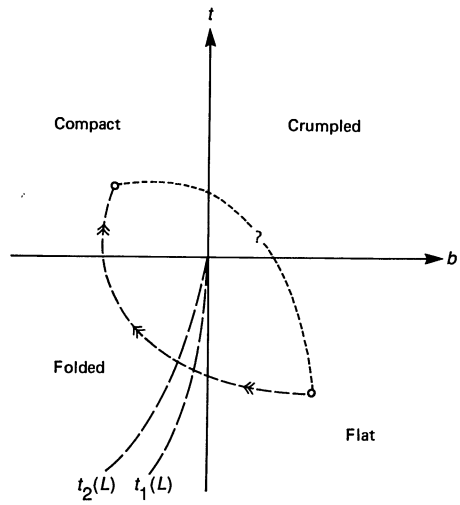

Fig. 3. Schematic phase diagram from a Landau theory. The arrows on the dotted line indicate the possible trajectory observed in simulations on cooling.

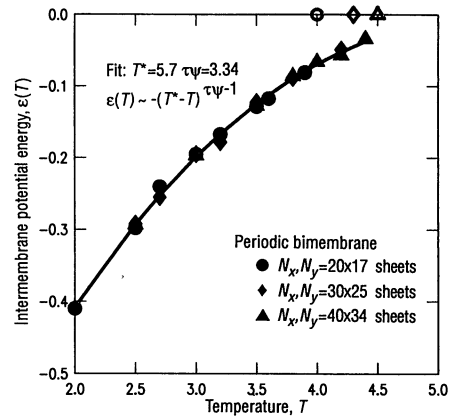

Fig. 4. The binding energy of bimembranes with periodic boundary conditions. The open symbols represent the unbinding temperature for each of the three membranes.

The unfolding of singly folded membranes bears close resemblance to the unbinding transition of two distinct surfaces (*7*); this is most easily seen if the membrane is cut at the crease. Unbinding and related wetting transitions (*17*) are characterized by two length scales. One is the average separation $\xi_\perp$ between the membranes, and the other is the in-plane size $\xi_\parallel$ of characteristic

fluctuations (blobs of separated membranes). The two length scales are related by the membrane roughness exponent; that is, $\xi_\perp \sim \xi_\parallel^\zeta$. Recent renormalization group (RG) studies (7) suggest that the unbinding of membranes is a continuous transition, $\xi_\parallel$ and $\xi_\perp$ diverge at the unbinding transition T^*, for example, $\xi_\perp \sim (T^* - T)^\psi$ diverges with an exponent ψ. Scaling arguments indicate that the binding free energy vanishes at the transition because $b(T) \sim \xi_\parallel^{-2} \sim (T^* - T)^{\tau\psi}$, where $\tau = 2/\zeta$. The RG estimate (7) is $\tau\psi \sim 2.7$.

Because this free-energy gain provides the driving force for the folding transition, it is important to examine its behavior. Hence we performed molecular dynamics simulations of the unbinding of two membranes. To minimize finite-size effects periodic boundary conditions were imposed, and to ensure that such boundary conditions do not squeeze or stretch the membrane the computational box was allowed to vary by means of a constant-pressure molecular dynamics technique until zero pressure was achieved. Then the computational box size was fixed. We found that 20 × 17 bimembranes unbind at $T_u(20) = 4.0$ and that 30 × 25 bimembranes unbind at $T_u(30) = 4.3$, whereas the 40 × 34 unbinding temperature $T_u(40) = 4.5$. The size dependence of the unbinding temperature was expected because finite membranes will unbind once the characteristic size of the disjointed blobs is on the order of the membrane size.

To obtain the scaling behavior, we measured the binding energy of bimembranes. The results are plotted in Fig. 4 and fitted to a power law such that $\epsilon(T) = \partial b/\partial T \sim -(T^* - T)^{\tau\psi - 1}$. We see that bimembranes of different size have the same binding energy until there is a drop to 0 at the unbinding temperature. From the fits we estimate that $T^* = 5.7$ and $\tau\psi = 3.34 \pm 0.16$. There is some quantitative discrepancy with the RG results, but more careful work is required to establish unambiguously the validity and universality (7) of the scaling behavior at this unbinding transition.

One interesting aspect of these results is that, although the folding transitions are closely spaced around $T \sim 3$, the unbinding transitions with period boundary conditions for similarly sized bimembranes occur at about a 30% higher temperature. For very large sizes the two transitions are expected to occur at the same point. This is partly because the binding free energy grows slowly with decreasing temperature [$\sim(T^* - T)^{3.33}$], and hence a low temperature is required to overcome the crease energy. We also examined the unbinding transition of a bimembrane of side 49 with free boundary conditions, however, and found that it unbinds at $T = 3.4 \pm 0.1$, which is closer to the folding temperature than the unbinding temperature of bimembranes with periodic boundary conditions. The crease energy cannot be invoked in this case, and another mechanism must be at work. From examination of configurations of membranes, such as those in Fig. 1, it becomes clear that the free edge of a membrane has quite strong fluctuations. These fluctuations are suppressed in the case of periodic boundary conditions and are also reduced when the membrane is folded.

We can estimate the free-energy cost associated with the loss of edge fluctuations. When one of the edge particles is pinned, it loses an entropy of roughly $\ln H$, where H is the typical width over which an unpinned particle fluctuates. Because the number of edge sites is proportional to L, the total entropy loss is proportional to L ($\ln H$). From the result $H \sim L^\zeta$ for membranes (*12, 14*), we conclude that a free-energy term from edge effects grows as $\zeta L(\ln L)$; that is, the growth is superlinear. Such superlinear growth is highly unusual because finite-size effects usually lead to linear corrections. Such logarithmic finite-size corrections are familiar in nucleation theory (*18*) and are clearly also important in fluctuating membranes.

Putting these elements together, we conclude that for $T < T^*$ the free energy Δf of a singly folded state for a membrane of size L, with respect to the flat state, scales as

$$\Delta f_1 = [-(T^* - T)^{\tau\psi} L^2] + \epsilon_c L + \alpha L(\ln L) \quad (3)$$

where α is a constant of order of unity (for the unbinding transition with open edges, the crease energy will be absent). For sufficiently big membranes the energy loss of creasing is actually irrelevant compared to the entropy loss of edge fluctuations. This is in part responsible for the closeness in the temperatures of folding and unbinding with open boundaries. The folding transition occurs when $\Delta f_1 = 0$, and hence

$$T_1(L) = T^* - \left[\alpha'\left(\frac{\ln L}{L}\right)\right]^{1/\tau\psi} \quad (4)$$

The folding transitions for $T_1(75) \sim 3.2$ and $T_1(49) \sim 2.9$ are roughly consistent with the above formula, although because these temperatures are two times smaller than T^* the scaling law cannot be precise. It is also because of these relatively low temperatures that the folds shown in Fig. 1 are so localized and straight. Presumably, close to T^* an artificially imposed crease will be rounded into a cylinder to minimize the cost in bending energy. Similar scaling forms are expected for the second and successive folding transitions. Finite-size effects will become progressively more important and involved, however, and a theory starting from the binding transition will quickly lose predictive power.

In summary, we have shown that attraction between flat membranes can lead to folding and unbinding transitions that are intimately linked. The binding free energy appears to vanish as $b(T) \sim (T^* - T)^{3.33}$ for infinite-sized membranes, whereas in finite membranes the free-energy loss due to edge fluctuations [$\sim L(\ln L)$] is also important. If solutions of tethered membranes can be prepared, such reversible transitions may lead to many novel applications. In dense solutions the membranes will stack together at T^*, forming a highly anisotropic solid (*19*), and in dilute solutions the membranes will fold on themselves at a temperature lower than T^*. These low-temperature states can provide a means of transporting small particles: Material trapped in the folds or in the stack can be safely moved with the surfaces and then released by going back to the original flat and unbound state. Theoretically, one can even design the shapes and morphologies of the low-temperature states by selectively introducing elements with attractive interactions. Abraham has conceived of a model membrane in which the attractive interaction is restricted to particles on the rim of the membrane (*20*). At sufficiently low temperature, molecular dynamic simulations show that the membrane folds and "zips" closed around the rim, resulting in a closed surface that is inflated as a result of self-avoidance among the interior membrane particles.

REFERENCES AND NOTES

1. Y. Kantor *et al.*, *Phys. Rev. Lett.* **57**, 791 (1986); *Phys. Rev. A* **35**, 3056 (1987).
2. D. R. Nelson, T. Piran, S. Weinberg, Eds., *Statistical Mechanics of Membranes and Interfaces* (World Scientific, Singapore, 1989).
3. P. G. de Gennes, *Scaling Concepts in Polymer Physics* (Cornell Univ. Press, Ithaca, NY, 1979).
4. D. R. Nelson and L. Peliti, *J. Phys.* (*Paris*) **48**, 1085 (1987).
5. Y. Kantor and D. R. Nelson, *Phys. Rev. Lett.* **58**, 2774 (1987); *Phys. Rev. A* **38**, 4020 (1987).
6. J. A. Aronovitz and T. C. Lubensky, *Phys. Rev. Lett.* **60**, 2634 (1988).
7. R. Lipowsky, *ibid.* **62**, 705 (1989); S. Grotehans and R. Lipowsky, *Phys. Rev. A* **41**, 4574 (1990).
8. M. Kardar and D. R. Nelson, *Phys. Rev. A* **38**, 966 (1988) and references therein.
9. M. Paczuski, M. Kardar, D. R. Nelson, *Phys. Rev. Lett.* **60**, 2638 (1988); F. David and E. Guitter, *Europhys. Lett.* **5**, 709 (1988); M. Paczuski and M. Kardar, *Phys. Rev. A* **39**, 6086 (1989).
10. M. Plischke and D. H. Boal, *Phys. Rev. A* **38**, 4943 (1988); F. F. Abraham, W. E. Rudge, M. Plischke, *Phys. Rev. Lett.* **62**, 1757 (1989); J.-S. Ho and A. Baumgartner, *ibid.* **63**, 1324 (1989).
11. M. A. F. Gomes and G. L. Vasconcelos, *Phys. Rev. Lett.* **60**, 238 (1988); Y. Kantor, M. Kardar, D. R. Nelson, *ibid.*, p. 239.
12. F. F. Abraham and D. R. Nelson, *Science* **249**, 393 (1990). An expanded version, with a discussion of

the compact phase, appears in *J. Phys. (Paris)* **51**, 2653 (1990).
13. T. Hwa, thesis, Massachusetts Institute of Technology (1990).
14. S. Leibler and A. C. Maggs, *Phys. Rev. Lett.* **63**, 406 (1989).
15. M. Kardar, *Nucl. Phys. B* **5A**, 209 (1988).
16. See, for example, (*1*) and references therein.
17. For example, see the review by S. Dietrich on wetting phenomena in *Phase Transitions and Critical Phenomena*, C. Domb and J. L. Lebowitz, Eds. (Academic Press, London, 1988), vol. 12, chap. 1.
18. F. F. Abraham, *Homogeneous Nucleation Theory* (Academic Press, New York, 1974), sect. 3.7 and chap. 6; _____ and J. Canosa, *J. Chem. Phys.* **50**, 1303 (1969).
19. J. Toner, *Phys. Rev. Lett.* **64**, 1741 (1990).
20. F. F. Abraham, in preparation.
21. We have benefited from conversations with D. R. Nelson. F.F.A. acknowledges a probing comment by J. S. Langer that led to the simulation of the "zipper" transition in the model membrane with attraction being restricted to the rim particles of the membrane. Research by M.K. was supported by NSF grant DMR-90-01519.

10 October 1990; accepted 14 January 1991

The Shapes and Sizes of Closed, Pressurized Random Walks

JOSEPH RUDNICK AND GEORGE GASPARI

Two-dimensional cell-like membranes acted on by osmotic pressure differentials are represented by closed, unrestricted random walks. The treatment omits excluded-volume effects, and the pressure that is imposed thus favors an oriented area, so that the shriveled configuration of a vesicle with excess external pressure is inaccessible in this model. Nevertheless, the approach has the decided advantage of yielding analytic expressions in a complete statistical analysis. Results are presented for the average square of the radius of gyration, the asphericity, and the probability distribution of the principal components of the radius of gyration tensor. The analysis is done in both the constant-pressure and constant-area ensembles.

TWO-DIMENSIONAL VESICLES, AS modeled by Leibler and colleagues (*1*), consist of closed, self-avoiding chains that encircle a two-dimensional volume. If one introduces a pressure differential between the enclosed volume and the region surrounding the vesicle, one has a model for cell-like structures subject to osmotic forces. Numerical studies reveal the existence of three different regimes of vesicle conformations and a catastrophic transition as the difference between the internal and the external pressure is varied (*2, 3*). When this difference is sufficiently large and negative, the vesicles become severely deflated. The walls of the shriveled vesicles resemble tree-like structures. In fact, the walls appear to be governed by the statistics of branched, excluded-volume polymers. When the pressure differential is close to zero, the vesicles are flaccid. The scaling laws governing the wall conformations are those of simple, closed, self-avoiding walks. As the pressure differential is increased to a sizable positive value, the vesicles inflate and increasingly resemble two-dimensional inflated balloons. At a critical value of the pressure differential, the vesicles share the fate of the overinflated balloon and explode, unless the walls are made of extremely rigid segments. These studies (*1–3*) also have investigated the shape distributions and scaling properties of vesicles and their walls in these three regimes.

We now report the results of calculations of a number of properties of two-dimensional vesicles with non–self-avoiding walls. We have discovered that removing the excluded-area restriction transforms the pressurized vesicle system from a model whose specific properties can only be obtained numerically to one that is completely solvable. We have obtained explicit expressions for various important properties, including the full combined distribution function for the principal radii of gyration of vesicles under the influence of excess internal pressure. We also have obtained results for vesicle sizes and shapes in the conjugate constant-area ensemble.

We investigated the scaling properties of the two-dimensional vesicle with non–self-avoiding walls and found that the scaling forms proposed by Leibler *et al.* (*1*) hold in the corresponding regimes of our simpler model. Although allowing vesicle walls to intersect ignores a fundamental physical restriction on the allowed conformations of real membranes, we hold that the extreme tractability of this model more than offsets the disadvantages resulting from the tenuousness of its connection to real, three-dimensional vesicles. In addition, we anticipate that the results reported here will be the zeroth-order results on which one can hope to improve with the use of the powerful new techniques that have been applied to various two-dimensional systems.

J. Rudnick, Department of Physics, University of California, Los Angeles, CA 90024.
G. Gaspari, Department of Physics, University of California, Santa Cruz, CA 95064.

The vesicles we studied have walls consisting of N linear links, or displacements, $\boldsymbol{\eta}_i$ ($1 \leq i \leq N$). The walls are closed, so that $\Sigma\boldsymbol{\eta}_i = 0$. The links are, in the absence of a pressure differential, governed by a simple Gaussian distribution in that the probability that the link $\boldsymbol{\eta}_i$ has a length between η and $\eta + d\eta$ is proportional to $\exp(-\eta^2)d\eta$. The influence of the pressure differential p is felt through the following additional contribution to the probability distribution:

$$P_A(\boldsymbol{\eta}_i) = e^{-pA} \quad (1)$$

where A is the oriented area of the closed wall; this is to say that A is given by the integral $\frac{1}{2}\oint(y\,dx - x\,dy)$ taken along the wall in the direction of increasing index i. Notice that if the vesicle is flipped over the area defined in this way changes sign. A vesicle with a higher pressure inside than outside will tend to inflate (in a particular sense). A vesicle with a negative pressure differential will inflate in the opposite sense. There is no deflated phase. Furthermore, "figure eight" and more complicated configurations in which the vesicle walls cross will occur. Thus in this model a pressure differential has the effect of discouraging "wrong" sense configurations.

The distribution function governing individual link lengths is also taken to be Gaussian. In this respect, the statistics of the bounding surface are those of a closed,

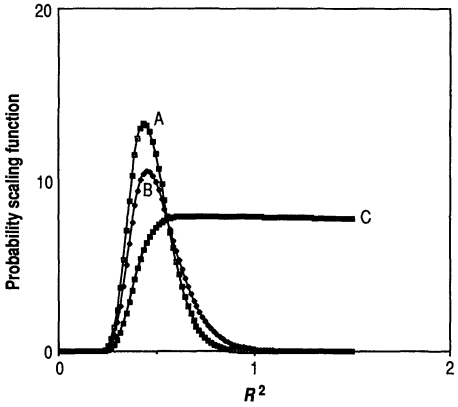

Fig. 1. Probability distribution scaling function, $\mathcal{P}(R^2N^{-2\nu}, x^{2\nu})$ (see Eq. 11), plotted against R^2 for (curve A) $p \ll p_c$, (curve B) $p = p_c/2$, and (curve C) $p = 0.999p_c$. The vertical scale is enhanced by a factor of 200 in the case of curve C.